

Theoretical Studies of the Mechanism of Aerobic Alcohol Oxidation with Palladium Catalyst Systems

Timofei Privalov,* Christian Linde, Krister Zetterberg, and Christina Moberg

Department of Chemistry, Organic Chemistry, Royal Institute of Technology,
SE 100 44 Stockholm, Sweden

Received November 8, 2004

Density functional theory (DFT) was applied to a comprehensive mechanistic study of the Pd(II)-catalyzed oxidation of alcohols by molecular oxygen. Both parts of the catalytic cycle, i.e., the oxidative dehydrogenation of the substrate and the regeneration of the catalyst by the co-oxidant, molecular oxygen, were studied. The catalytic cycle under consideration consists of intramolecular deprotonation, β -hydride elimination, and migratory insertion steps, and it is relevant for a wide class of catalytic systems. In particular, a Pd(II) cyclometalated system was addressed and qualitatively compared with the Uemura system (Pd(OAc)₂/pyridine) and with the Pd–carbene system. Geometries of the intermediate complexes and relative Gibbs free energies were identified along the proposed reaction path with the help of computational methods. The transition state for the β -hydride elimination, which is the highest point on the energy profile of the catalytic cycle, was identified.

1. Introduction

Aerobic palladium-catalyzed oxidations of primary and secondary alcohols to aldehydes and ketones, respectively, have emerged as powerful atom-efficient processes, producing only nonhazardous byproducts.¹ Several catalytic systems consisting of a Pd(II) catalyst precursor, commonly Pd(OAc)₂, and DMSO² or a nitrogen-containing ligand such as pyridine,³ triethylamine,⁴ a phenanthroline derivative⁵ or sparteine,⁶ have been employed for the process. We recently found that cyclopalladated imine complexes in the presence of pyridine serve as efficient catalysts for oxidations employing oxygen in air at ambient pressure as the stoichiometric oxidant,⁷ and later it was found that carbene complexes can be used for oxidations under similar conditions.⁸

Several mechanistic studies of palladium-catalyzed aerobic alcohol oxidations, experimental as well as theoretical, have been reported. An experimental study of the mechanism of Uemura's Pd(OAc)₂/pyridine system suggested initial formation of a palladium(II) alkoxide containing two molecules of pyridine along with acetic acid, followed by the dissociation of one pyridine ligand and final β -elimination.⁹ Substrate oxidation by Pd(II) was shown to be turnover limiting with this catalytic system, implying a Pd(II) resting state. This is in contrast to the less active Pd(OAc)₂/DMSO system, which features turnover-limiting oxidation of Pd(0).¹⁰ Recently gas-uptake kinetic methods and ¹H NMR spectroscopy were employed for a comprehensive study of the mechanism of the catalytic oxidation of benzyl alcohol in the Pd(OAc)₂/pyridine system.¹¹ This study confirmed the previously proposed reaction mechanism. In particular, the in situ spectroscopic data revealed that the first step of the reaction is the formation of an adduct between the alcohol and Pd(II). The reaction was shown to then proceed via coupled proton transfer and ligand substitution, transformation of the alkoxide species to a three-coordinated intermediate via dissociation of pyridine, and finally irreversible β -hydride elimination to produce benzaldehyde. Most recently, the interaction of molecular oxygen with Pd(0) species has been studied theoretically.¹²

The purpose of this paper is to present a computational study of the palladium-catalyzed transformation of an alcohol to a carbonyl compound, namely the oxidation of 1-phenylethanol catalyzed by the recently developed palladacycle **1**, and to compare the mechanism with that of the Pd(OAc)₂ system.

* To whom correspondence should be addressed. E-mail: priti@kth.se.

(1) (a) Muzart, J. *Tetrahedron* **2003**, *59*, 5789–5816. (b) Stahl, S., *Angew. Chem., Int. Ed.* **2004**, *43*, 3400–3420.

(2) (a) Peterson, K. P.; Larock, R. C. *J. Org. Chem.* **1998**, *63*, 3185–3189. (b) van Benthem, R. A. T. M.; Hiemstra, H.; van Leeuwen, P. W. N. M.; Geus, J. W.; Speckamp, W. N. *Angew. Chem., Int. Ed. Engl.* **1995**, *34*, 500–503.

(3) (a) Nishimura, T.; Onoue, T.; Ohe, K.; Uemura, S. *Tetrahedron Lett.* **1998**, *39*, 6011–6014. (b) Nishimura, T.; Onoue, T.; Ohe, K.; Uemura, S. *J. Org. Chem.* **1999**, *64*, 6750–6755. (c) Nishimura, Y.; Maeda, Y.; Kakiuchi, N.; Uemura, S. *J. Chem. Soc., Perkin Trans. 1* **2000**, 4301–4305.

(4) Schultz, M. J.; Park, C. C.; Sigman, M. S. *Chem. Commun.* **2002**, 3034–3035.

(5) (a) Bianchi, D.; Bortolo, R.; D'Aloisio, R.; Ricci, M. *Angew. Chem., Int. Ed.* **1999**, *38*, 706–708. (b) ten Brink, G.-J.; Arends, I. W. C. E.; Sheldon, R. A. *Science* **2003**, *287*, 1636–1639.

(6) (a) Jensen, D. R.; Pufsfley, J. S.; Sigman, M. S. *J. Am. Chem. Soc.* **2001**, *123*, 7475–7476. (b) Ferreira, E. M.; Stoltz, B. M. *J. Am. Chem. Soc.* **2001**, *123*, 7725–7726. (c) Nielsen, R. J.; Keith, B. M.; Goddard, W. A. *J. Am. Chem. Soc.* **2004**, *126*, 7967–7974.

(7) (a) Hallman, K.; Moberg, C. *Adv. Synth. Catal.* **2001**, *343*, 260–263. (b) Paavola, S.; Zetterberg, K.; Privalov, T.; Csöreg, I.; Moberg, C. *Adv. Synth. Catal.* **2004**, *346*, 237–244.

(8) (a) Jensen, D. R.; Schultz, M. J.; Mueller, J. A.; Sigman, M. S. *Angew. Chem. Int. Ed.* **2003**, *42*, 3810–3813. (b) Jensen, D. R.; Sigman, S.; Matthew, *Org. Lett.* **2003**, *5*, 63–65. (c) Mueller, J. A.; Goller, C. P.; Sigman, S. M. *J. Am. Chem. Soc.* **2004**, *126*, 9724–9734.

(9) Steinhoff, B. A.; Stahl, S. S. *Org. Lett.* **2002**, *4*, 4179–4181.

(10) Steinhoff, B. A.; Fix, S. R.; Stahl, S. S. *J. Am. Chem. Soc.* **2002**, *124*, 766–767.

(11) Steinhoff, B. A.; Guzei, I. A.; Stahl, S. S. *J. Am. Chem. Soc.* **2004**, *126*, 11268–11278.

(12) Landis, C. R.; Morales, C. M.; Stahl, S. S. *J. Am. Chem. Soc.* **2004**, ASAP.

2. Computational Details

The calculations of the mechanisms for catalytic alcohol oxidation were performed in three steps. First, geometry optimizations of all intermediate complexes and transition states were carried out using the B3LYP functional¹³ with the lacvp*/6-31G(d) basis set.^{14,15} Double- ζ basis sets with additional polarization functions are known to give good optimized structures with accurate description of the interaction of ligands with the transition metal. All degrees of freedom were optimized, and only positive vibrational frequencies were obtained at the optimized geometries, even in the case of the displaced and loosely bound ligands. Transition states obtained were characterized by the presence of exactly one imaginary vibrational frequency along the appropriate normal mode.

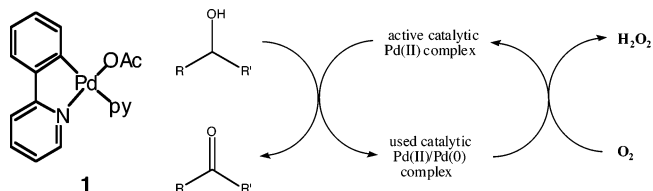
In the second step, B3LYP energies were computed for the optimized geometry using a much larger triple- ζ basis, lacv3p*+/6-311+G(d), with additional diffuse and polarization functions. To account for the open-shell electrons in the high-spin Pd–O₂ complexes, an unrestricted DFT methodology, UB3LYP, was employed. All computations were performed with the Jaguar v4.0 suite of ab initio quantum-chemistry programs.¹⁶ Solvent (toluene) was represented with the following parameters: $\epsilon = 2.379$ and probe radius $r_p = 2.762$ Å. Gas-phase-optimized structures were used in the solvation calculations within the self-consistent reaction field model as implemented in the Jaguar computational package.

Finally, complete thermochemical analysis and additional transition-state search were performed with the Gaussian 98¹⁷ computational package within the restricted/unrestricted B3LYP level of theory and with the LanL2DZ¹⁴ basis set. The structures of the intermediate complexes and transition states were reoptimized with this basis set prior to the computation of harmonic vibrational frequencies at the B3LYP/LanL2DZ level. The use of the effective potential LanL2DZ basis set for thermochemical analysis, namely for acquiring thermodynamic functions and Gibbs free energy, has regularly been found to result in a level of accuracy comparable to that of superior basis sets at a small fraction of the computational cost.

3. Mechanistic and Computational Models for the Catalytic Dehydrogenation with Cyclopalladated 2-Phenylpyridine as Catalyst

In our previous communication we applied computational methods to studies of the bridge-splitting reaction to form the monomeric square-planar Pd(II) heterocyclic complex **1** (Scheme 1) and the ligand exchange reactions with pyridine, water, and alcohol molecules.^{7b} Ab initio calculations, with the account of solvent effects, unambiguously indicated that pyridine is energetically pre-

Scheme 1. Square-Planar Pd Heterocycle, Palladacycle **1**, with a Pyridine (py) Ligand and Illustration of the Catalytic Oxidation of an Alcohol: (Left) Interaction of the Substrate with the Catalyst and Oxidation Reaction; (Right) Reduction of Molecular Oxygen and Regeneration of the Pd Catalyst to the Active State



ferred as a ligand over the substrate (1-phenylethanol) or water. NMR spectroscopic studies at room temperature of the addition of pyridine, water, or acetic acid to the initial dimeric acetate-bridged complex revealed that only pyridine was able to split the acetate bridge and that pyridine was not replaced by added 1-phenylethanol, thus confirming the theoretical results.¹⁸

Oxidation of an alcohol catalyzed by Pd complexes involves two redox processes. The left cycle of Scheme 1 shows the oxidation of the alcohol by palladacycle **1**. Two proton transfers are required for the alcohol to be transformed to the product aldehyde or ketone. According to the great volume of experimental information, molecular oxygen does not participate in this part of the reaction. Instead, molecular oxygen interacts with the Pd complex after the formation of the final carbonyl product, thus regenerating the catalyst in its active state and at the same time producing hydrogen peroxide.

Depending on the ligand arrangement in the Pd complex, the metal ion may change oxidation state from II to 0 and back in the course of the reaction. The heterocycle ligand in palladacycle **1** carries a formal negative charge due to the C–Pd bond. Under the assumption that Pd(II) remains coordinated to this ligand throughout the reaction and that one additional ion (AcO[−]) with negative charge is coordinated to Pd, the oxidation state of the metal center will remain constant through the reaction pathway presented in Scheme 1, or anionic complexes need to be formed. The low dielectric constant of the solvent, $\epsilon = 2.379$, does not favor formation of charged complexes along the reaction pathway.¹⁹ In addition, anionic σ -palladium complexes would probably require ligands with better π -accepting properties.

3.1. Binding of Substrate to the Catalytic Complex. Coordination of the substrate molecule to the Pd catalyst is the first step of the oxidation reaction, and therefore it is instructive to find similarities in the binding of different substrates to the most commonly employed catalytic systems, i.e., Pd(*i*Pr)(OAc)₂ and Pd(OAc)₂(pyridine)₂, and the newly developed palladacycle **1** catalyst.

Pd(*i*Pr)(OAc)₂. The DFT-optimized structure of the Pd(*i*Pr)(OAc)₂–methanol complex (see Figure 1A and Scheme 2) shows the substrate, methanol, binding to Pd via the O–H bond, which is 1.52 Å long, while the Pd–O bond length is 2.14 Å. Smaller molecules, for

(13) (a) Becke, A. D. *J. Chem. Phys.* **1993**, *98*, 5648. (b) Lee, C.; Yang, W.; Parr, R. G. *Phys. Rev. B* **1988**, *37*, 785–789.

(14) Hay, P. J.; Wadt, W. R. *J. Chem. Phys.* **1985**, *82*, 299–310.

(15) (a) Hehre, W. J.; Ditchfield, R.; Pople, J. A. *J. Chem. Phys.* **1972**, *56*, 2257–2261. (b) Francl, M. M.; Pietro, W. J.; Hehre, W. J.; Binkley, J. S.; Gordon, M. S.; Defrees, D. J.; Pople, J. A. *J. Chem. Phys.* **1982**, *77*, 3654–3665. (c) Hariharan, P. C.; Pople, J. A. *Theor. Chim. Acta* **1973**, *28*, 213–222.

(16) Jaguar 4.0; Schrödinger, Inc., Portland, OR, 1991–2000.

(17) Frisch, M. J.; Trucks, G. W.; Schlegel, H. B.; Scuseria, G. E.; Robb, M. A.; Cheeseman, J. R.; Zakrzewski, V. G.; Montgomery, J. A. Jr.; Stratmann, R. E.; Burant, J. C.; Dapprich, S.; Millam, J. M.; Daniels, A. D.; Kudin, K. N.; Strain, M. C.; Farkas, O.; Tomasi, J.; Barone, V.; Cossi, M.; Cammi, R.; Mennucci, B.; Pomelli, C.; Adamo, C.; Clifford, S.; Ochterski, J.; Petersson, G. A.; Ayala, P. Y.; Cui, Q.; Morokuma, K.; Malick, D. K.; Rabuck, A. D.; Raghavachari, K.; Foresman, J. B.; Cioslowski, J.; Ortiz, J. V.; Baboul, A. G.; Stefanov, B. B.; Liu, G.; Liashenko, G.; Piskorz, P.; Komaromi, I.; Gomperts, R.; Martin, R. L.; Fox, D. J.; Keith, T.; Al-Laham, M. A.; Peng, C. Y.; Nanayakkara, A.; Challacombe, M.; Gill, P. M. W.; Johnson, B.; Chen, W.; Wong, M. W.; Andres, J.; Gonzalez, C.; Head-Gordon, M.; Replogle, E. S.; and Pople, J. A.; *Gaussian 98*, Revision A.9; Gaussian, Inc., Pittsburgh PA, 1998.

(18) Moberg, C.; Paavola, S.; Zetterberg, K. Unpublished results.

(19) No oxidation was observed in methylene chloride, acetonitrile, or tetrahydrofuran.

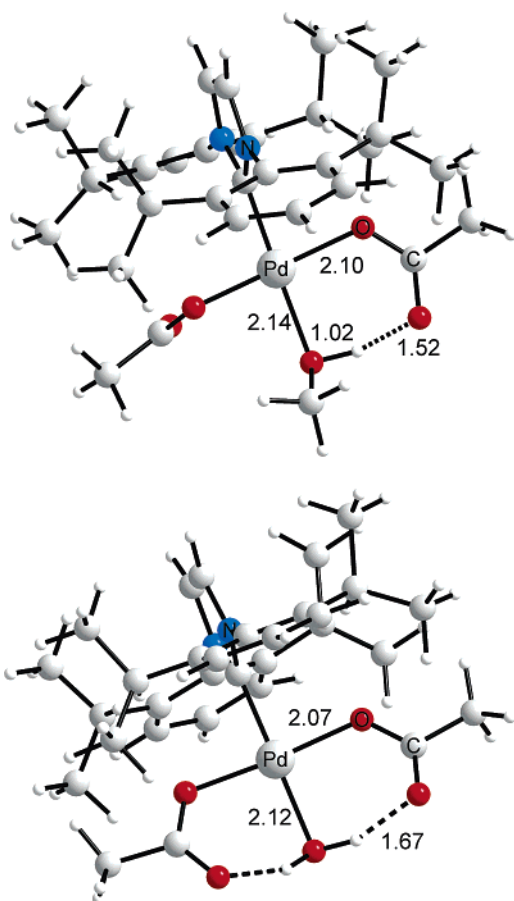
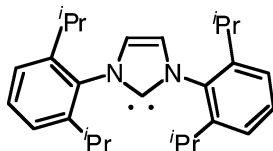


Figure 1. DFT-optimized structures of the Pd(IiPr)(OAc)₂ complexes with methanol and water molecules coordinated to Pd: (A, top): Pd(IiPr)(OAc)₂-methanol complex; (B, bottom) Pd(IiPr)(OAc)₂-water complex. All bond distances are in Å.

Scheme 2. Scheme of the IiPr Ligand



example water, are able to participate in hydrogen bonding to both AcO units. The O-H bond length was found to be 1.67 Å, similar to that for the alcohol binding.

Pd(AcO)₂(pyridine)₂. Computations show that the most preferable coordination of benzyl alcohol to Pd^{II}-(OAc)₂(pyridine)₂ is that with a strong O-H bond of 1.8 Å (see Figure 2A) without replacement of pyridine or AcO⁻. An alternative way to form the complex undergoing oxidation is to bind the substrate directly to Pd, as shown in Figure 2B (the corresponding O-H bond is 1.51 Å).

It turns out that second-sphere coordination of the substrate is more favorable by almost 10 kcal/mol than direct coordination of the substrate to the Pd center with replacement of pyridine.²⁵ However, the substrate/pyridine ligand exchange becomes almost thermoneutral with the account of the thermochemical corrections to the Gibbs free energies, which is in agreement with experimental data.¹¹

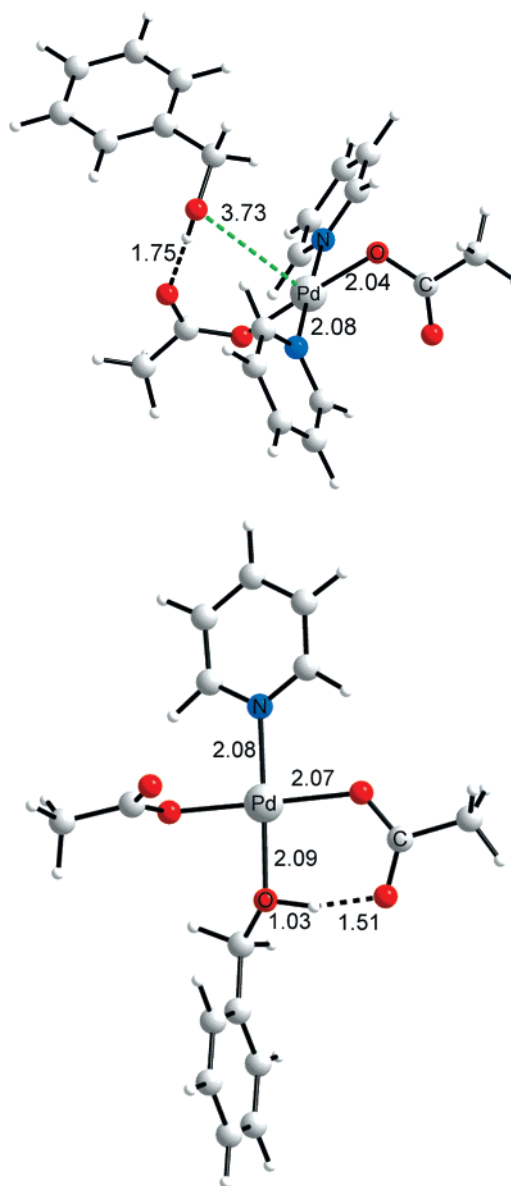


Figure 2. Pd-(OAc)₂-(pyridine)_N-substrate complexes: (A, top) *N* = 2; (B, bottom) *N* = 1. The green dashed line indicates the Pd-O distance. All bond distances are in Å.

Palladacycle 1. The substrate may coordinate to Pd either by direct means or via initial hydrogen bonding to the acetate group on Pd without replacement of pyridine from the coordination site (Figure 3 and Scheme 3, step 2A or 2B). Removal of pyridine from the coordination site of Pd requires energy, and therefore the substrate may bind via an O-H interaction to the AcO, resulting in an O-H bond length of 1.74 Å. The substrate may also bind to the vacant site on Pd with an O-Pd bond distance of 2.27 Å. Binding of the substrate in the second coordination sphere is more favorable by 7 kcal/mol in the gas phase and by 4.4 kcal/mol within PCM. An important feature of the adduct complexes is an O-H bond between the substrate and the oxygen atom of AcO; DFT geometry optimization predicts an O-H bond length of 1.59 Å.

Our computational results for three different catalysts with the AcO⁻ ion coordinated to Pd support the idea that the substrate preferably binds in the second coordination sphere. An O-H bond between the hydro-

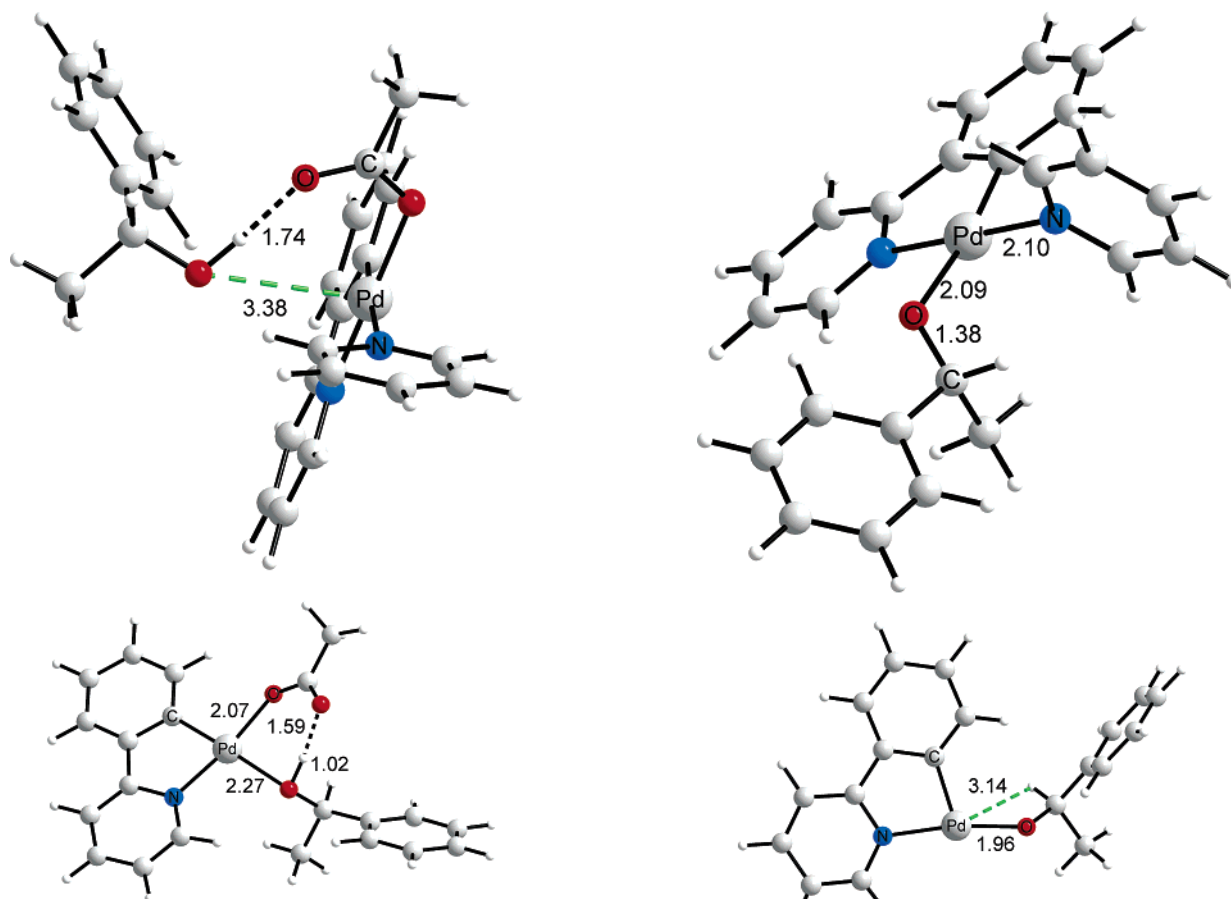


Figure 3. Coordination of substrate to palladacycle **1**: (A, top) coordination to the AcO via the O–H interaction (O–H bond is 1.74 Å); (B, bottom) direct coordination to Pd. The green dashed line indicates the Pd–O distance. All bond distances are in Å.

gen atom on the alcohol and the oxygen atom of the AcO ion is the common theme in all aforementioned cases. The presence of AcO[−] directs the oxidation reaction along this path of the proton transfer, the first step of the dehydrogenation reaction, regardless of the composition of the Pd catalyst.

3.2. Oxidation Part of the Cycle in the Four-Coordinated Pd(II) Model. The oxidation of the alcohol (left part of Scheme 1) is assumed to begin after the coordination of the substrate to palladacycle **1**.

From the first deprotonation step, the reaction proceeds with dissociation of AcOH from the coordination site of Pd (Scheme 3, step 3A). The binding energy of pyridine in the palladium–alkoxide complex (Figure 4A), without account of thermal corrections (only the electronic part), is −17 kcal/mol. However, comparison of the Gibbs free energies of the system with and without pyridine coordinated shows that thermodynamically pyridine is unbound. A complex with three-coordinated Pd is thermodynamically favored by a few kcal/mol.

The intermediate complex (Figure 4B) with the three-fold-coordinated palladium is 9 kcal/mol higher in energy than the β -hydride complex with the ketone (Figure 4C). It is technically straightforward to locate the transition state for the β -hydride elimination by comparing the threefold precursor (Figure 4B) with the fourfold successor (Figure 4C).

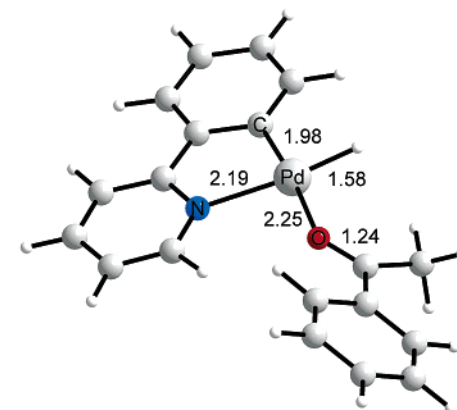
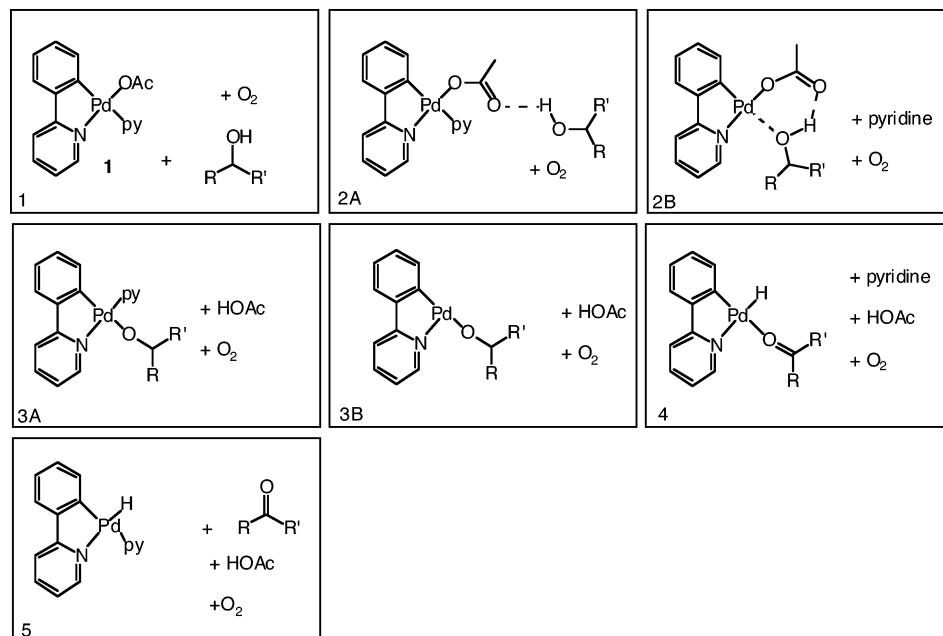


Figure 4. Key intermediate complexes along the alcohol oxidation (oxidative dehydrogenation) path of the catalytic cycle (see steps 3A,B and 4, Scheme 2): (A, top) precursor to the β -hydride elimination (four-coordinated Pd(II) intermediate); (B, middle) precursor to the β -hydride elimination with three-coordinated Pd; (C, bottom) intermediate complex of palladium with the carbonyl product. All bond distances are in Å.

Formation of the free carbonyl compound terminates the alcohol oxidation part of the catalytic cycle. According to the computed Gibbs free energies there is substantial driving force in the replacement of carbonyl by pyridine.

3.3. Transition State of the β -Hydride Elimination Process of Palladacycle **1.** The transition state with a hydrogen atom shared by Pd and carbon (Figure 5B) was identified. Calculation of the Hessian at the TS geometry revealed only one imaginary frequency

Scheme 3. Outline of the Four-Coordinated Pd Intermediate Complexes for the Oxidation of Alcohol Catalyzed by Palladacycle 1^a



^a In 2A and 2B, the substrate (alcohol) molecule may interact via O–H bonding only with the AcO unit without coordination to Pd (A), or it might replace pyridine and coordinate to Pd (B). In 3A and 3B, the intermediate complex from step 3A has four coordination sites occupied. In order for the β -hydride elimination to occur, decoordination of pyridine is required, opening the path for the movement of the hydrogen (see later in the text).¹¹ py = pyridine.

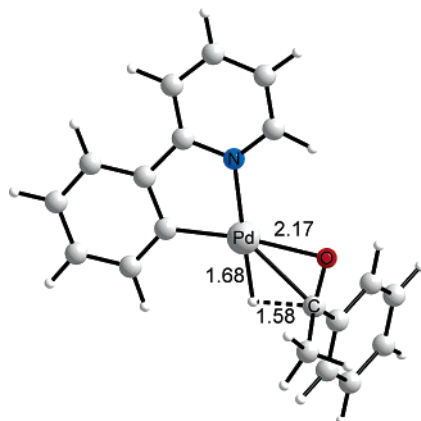


Figure 5. Transition state for the β -hydride elimination. All bond distances are in Å.

that corresponds to the distinctive movement of the hydrogen atom between Pd and C with additional small movements of the C, O, and Pd atoms (see the TIFF file with the animation of the corresponding normal mode in the Supporting Information). In the precursor complex (see Figure 4B) the Pd–O distance is 1.96 Å and the distance between Pd and H or C is slightly longer than 3.1 Å. In the transition state, the Pd–H distance is 1.68 Å and the H–C distance is 1.58 Å. The hydrogen atom is shared between the Pd and C atoms. The Pd–O distance is 2.17 Å, larger than in the precursor, but the Pd–C distance is shortened to 2.45 Å. During the proton transfer, the phenyl group rotates almost 180° clockwise.

A transition state of similar structure was reported recently by Mueller et al.^{8c} for the Pd(*i*Pr)(OAc)₂ system, though with a much longer hydrogen–carbon bond, (1.97 Å); the reported scenario of the β -hydride elimination also included a three-coordinated Pd inter-

mediate. Nielsen et al.^{6c} have computationally studied the oxidation of alcohols with the ((–)-sparteine)PdCl₂ system, and they reported a Pd–alkoxide intermediate and a β -hydride elimination transition state with very similar geometrical parameters, such as Pd–O, Pd–H, and H–C distances, as for the aforementioned transition state from Figure 5B.

4. Qualitative Description of the β -Hydride Elimination Process of Pd(AcO)₂(pyridine)₂: Intermediate Complexes and Transition State

A similar β -hydride elimination path was identified in the oxidation using the Pd^{II}(AcO)₂(pyridine)₂ system. Intermediate complexes and the transition state are presented within the most simple model of four-coordinated Pd (see Figure 6).

Interaction of the substrate, benzyl alcohol, with AcO[–] via an O–H bond (1.51 Å long, see Figure 2) leads to the first deprotonation of the substrate and formation of the three-coordinated Pd intermediate. The DFT-optimized geometry of the three-coordinated precursor (Figure 6A) has the following key parameters: the Pd–O distance is 1.94 Å, the Pd–C distance is 3.01 Å, and the shortest Pd–H distance is 3.03 Å. Optimization of the transition-state geometry (saddle point on the potential surface with strictly one imaginary frequency) was successful (see Figure 6B). The Gibbs free activation energy and the energy difference between precursor and transition state (see Figure 2 and Figure 6B, respectively) is 19.6 kcal/mol.²⁶ We found that the hydrogen atom is shared between Pd and carbon (compare with the transition state for the palladacycle **1** in Figure 5), that the Pd–O distance is 2.09 Å and the Pd–C distance is 2.43 Å, and that the Pd–H and C–H distances are 1.66 and 1.62 Å, respectively. We wish to point out our remarkable agreement with the corresponding bond

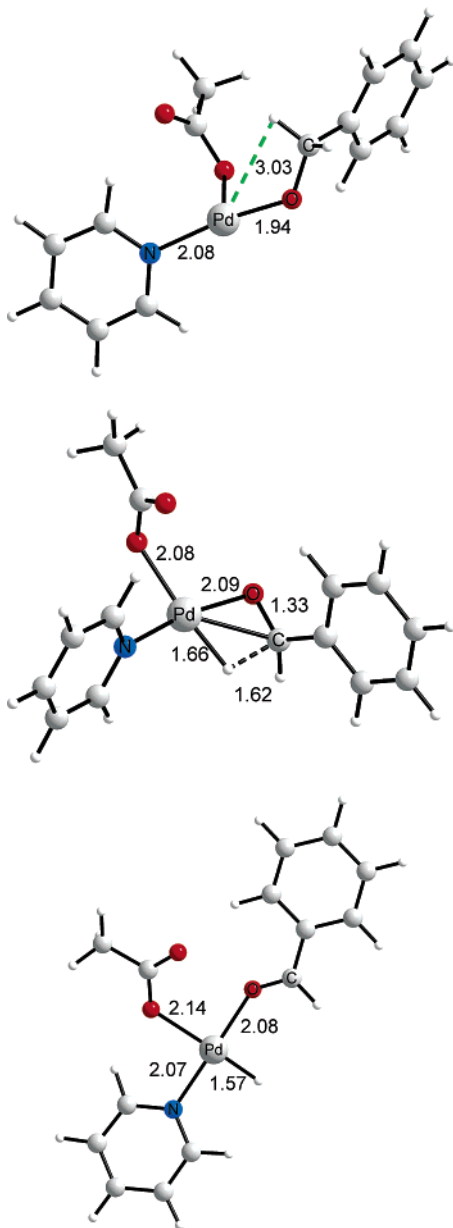


Figure 6. Simplified dehydrogenation path in the Pd^{II}-(AcO)₂(pyridine)₂ system: (A, top) intermediate three-coordinated Pd complex (the green dashed line indicates the shortest Pd–H distance); (B, middle) transition state; (C, bottom) Pd–hydride complex with the oxidized substrate. All bond distances are in Å.

distances in the transition-state structure for the ((-)-sparteine)PdCl₂ system.^{6c} The Pd–H bond length is 1.57 Å in the square-planar Pd–hydride complex (Figure 6C).

5. Interaction of O₂ with Pd Hydride

Coordination of molecular oxygen to Pd(II) opens up the possibility for migratory insertion, which we believe results in formation of HOO⁻ (part 7, Scheme 3). Finally, AcOH may coordinate to Pd(II) and readily deliver a proton to form hydrogen peroxide (H₂O₂). Hydrogen peroxide will be replaced by pyridine and the catalytic cycle will close up with the product (ketone or aldehyde) formed.

Three principally different mechanisms have been considered for the Pd-catalyzed aerobic oxidations.^{1b}

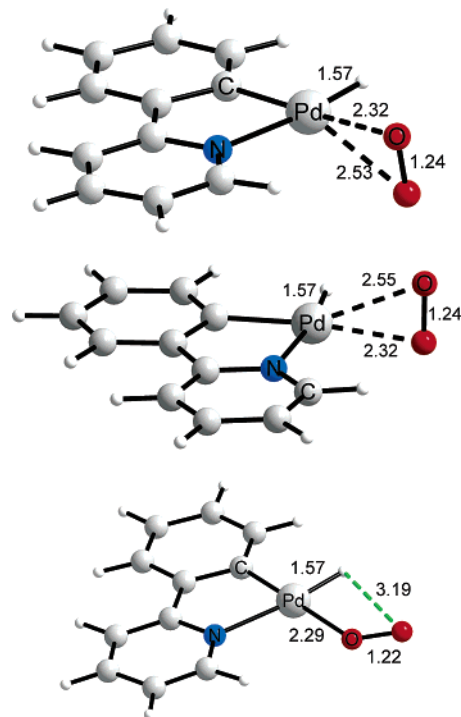


Figure 7. Binding of molecular oxygen to palladium hydride: (A, top; B, middle) two η^1 -intermediate complexes with the O₂ molecule pointing down and up, respectively, from the plane of the ligand; (C, bottom) planar η^1 -intermediate Pd–O₂ complex (the green dashed line indicates O–H distance). All bond distances are in Å.

Two of these involve the addition of O₂ to Pd(0) to yield a cyclic peroxopalladium(II) complex, while in the third mechanism Pd remains in the +2 oxidation state. The existence of a peroxo complex has been demonstrated experimentally by spectroscopy and X-ray crystallography,²⁰ and (η^2 -peroxo)palladium(II) complexes were recently studied theoretically.¹²

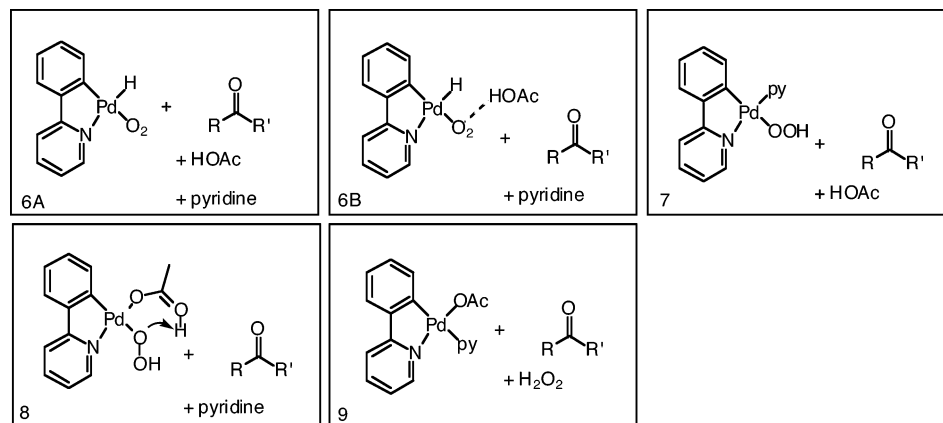
In contrast to the situation in Pd(II)/phenanthroline systems,²¹ a reaction pathway involving insertion of O₂ in a Pd(II) hydride is assumed to be preferred over addition of O₂ to a Pd(0) species with the present catalytic system. Pyridine may in principle act only as a base for the deprotonation of palladium hydride, but that would formally result either in charged intermediates or in a doublet ground electronic state of an η^2 -O₂–Pd complex. Furthermore, a pyridine–H complex would also be a doublet. Computational studies of such complexes require multiconfigurational (MCSCF) methods that account for spin–orbit effects, and they are out of the scope of the present study. In our present study we keep a focus on spin catalysis paths, suggesting that molecular oxygen coordinates to the available coordination site in the palladium–hydride complex (steps 6A,B, Scheme 4).

The ground electronic state of oxygen is known to be paramagnetic with two unpaired electrons. Due to the strong spin–orbit coupling, transition–metal reactions are weakly spin forbidden.²²

(20) (a) Stahl, S. S.; Thorman, J. L.; Nelson, R. C.; Kozee, M. A. *J. Am. Chem. Soc.* **2001**, *123*, 7188–7189. (b) Konnick, M. M.; Guzei, I. A.; Stahl, S. S. *J. Am. Chem. Soc.* **2004**, *126*, 10212–10213.

(21) (a) Stahl, S. S.; Thorman, J. L.; Nelson, R. C.; Kozee, M. A. *J. Am. Chem. Soc.* **2001**, *123*, 7188–7189. (b) ten Brink, G.-J.; Arends, I. W. C. E.; Sheldon, R. A. *Adv. Synth. Catal.* **2002**, *344*, 355–369.

Scheme 4. Continuation of Scheme 2: Participation of Molecular Oxygen in the Regeneration of the Pd Catalyst and Formation of Hydrogen Peroxide^a



^a In 6A and 6B are given two possible Pd–hydride–O₂ intermediate complexes with free AcOH (A) and with the AcOH unit bound to molecular oxygen via O–H interaction (B). py = pyridine.

We have found that molecular oxygen coordinates to the Pd(II) hydride complex in an η^1 manner. Two enantiomeric intermediate complexes with the O₂ molecule located almost perpendicular to the plane of the ligand were found (Figure 7A,B). The optimized ground electronic state of the Pd–O₂ intermediates is a triplet; the singlet configuration is 7.7 kcal/mol higher (UB3LYP/lacv3p**+++) in energy. The spin projection correction at the high-spin state,^{23,24} that is the separation between $S = 1$ and $S = 0$, increases the energy of the open shell singlet by almost 8 kcal/mol. Thus, the spin-corrected singlet–triplet splitting in the Pd–peroxo complexes is somewhat smaller than the singlet–triplet splitting in molecular oxygen (22 kcal/mol, see ref 23). In the palladium–hydride–oxygen complex (Figure 7A,B) the Pd–O distances are 2.32 and 2.53 Å and the O–O bond distance is 1.24 Å, 0.03 Å larger than the known equilibrium bond length³ in molecular oxygen, which is 1.21 Å. We have also identified the O₂–Pd intermediate complex with the O₂ molecule located in the plane of the ligand with only one oxygen atom bound to Pd (see Figure 7C). The Pd–O bond distances are 2.29 and 3.21 Å. This complex is less than 1 kcal/mol higher in energy than intermediates with the out-of-plane coordination of O₂. A η^2 transition state which connects “up” and “down” Pd–O₂ intermediates from Figure 7 was identified. An activation energy of less than 1 kcal/mol is required for the transformation between “up” and “down” coordination. In the transition state the O₂ molecule is perpendicular to the plane of the ligand and both oxygen atoms are coordinated to Pd.

7. Regeneration of the Catalyst: Formation of H₂O₂

The intermediate Pd–O₂ complex with planar or perpendicular coordination of molecular oxygen suggests a direct path for the proton transfer from Pd to O. Proton transfer to O₂ results in HOO[−] coordinated to

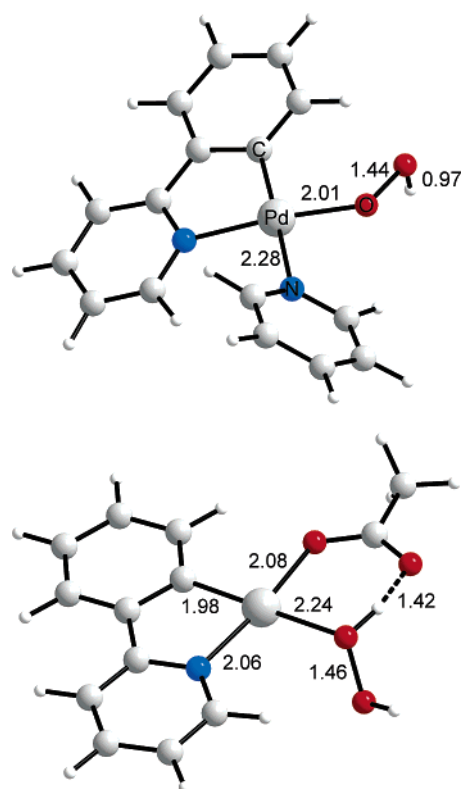


Figure 8. Restoration part of the catalytic cycle with the formation of H₂O₂: (A, top) intermediate complex with HOO[−]; (B, bottom) intermediate complex with H₂O₂. All bond distances are in Å.

palladium (see Figure 8A; pyridine fills in the vacant coordination site after the hydrogen is moved to the O–O group). The lowest energy electronic configuration of this complex was found to be a singlet with a Pd–O bond of 2.01 Å and an O–O distance of 1.44 Å, being 0.2 Å longer than the equilibrium O–O bond length, apparently due to the binding of hydrogen.

Stable analogues of the intermediate depicted in Figure 5A with AcOH instead of pyridine were not found. According to the calculations, there is a driving force for the transformation of AcOH to AcO[−] upon coordination to Pd during the geometry optimization. Optimization of the intermediate with the O–H bond

(22) Schwarz, H. *Int. J. Mass Spectrosc.* **2004**, 237, 75–105.

(23) Prabhakar, R.; Siegbahn, P. E. M.; Minaev, B. F.; Ågren, H. *J. Phys. Chem. B* **2002**, 106, 3742–3750.

(24) Mouesca, J.-M.; Chen, J. L.; Noodleman, L.; Bashford, D.; Case, D. A. *J. Am. Chem. Soc.* **1994**, 116, 11898–11914.

(25) Electronic energy only.

(26) The electronic only activation energy is 7.1 kcal/mol.

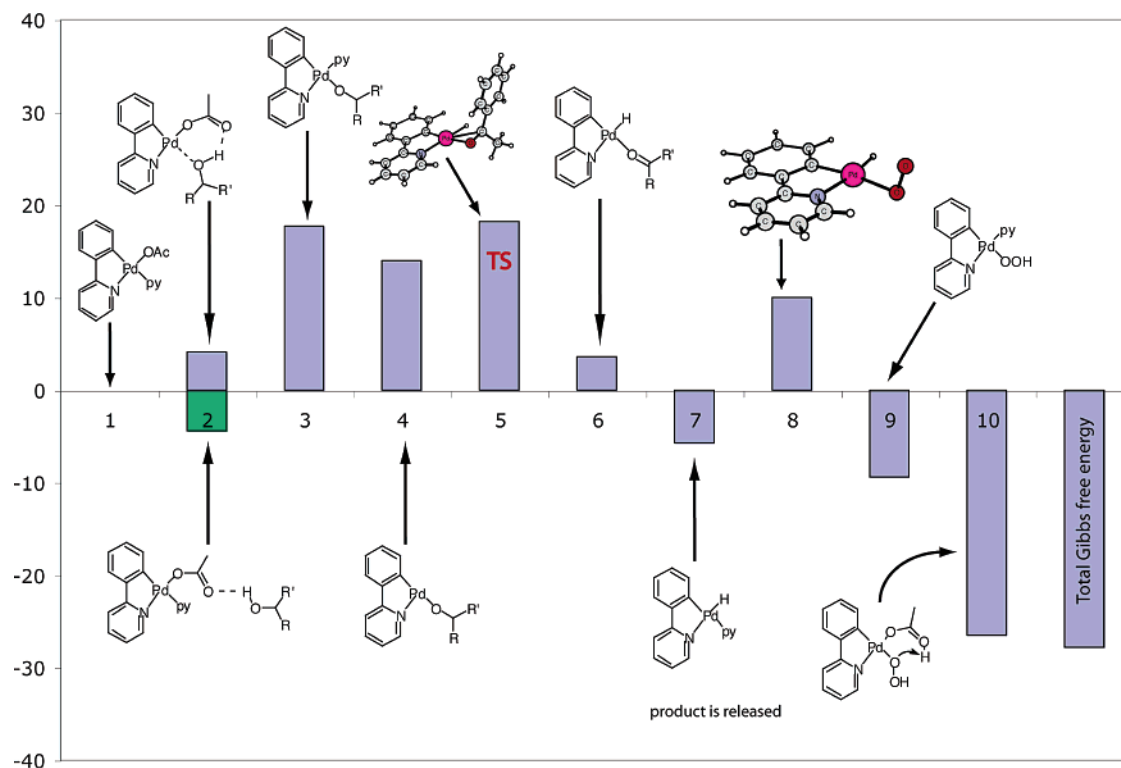


Figure 9. Gibbs free energy diagram for 1-phenylethanol oxidation in toluene: (y axis) relative Gibbs free energy of the reaction (kcal/mol); (x axis) reaction steps (see Table 1 for more details). R = Me, R' = Ph, py = pyridine. Schematic drawings show intermediate Pd complexes for each reaction step; the 3D structure of the β -hydride elimination transition state and Pd–O₂ complex is shown.

Table 1. Relative Electronic Energies along the Reaction Path Proposed in Scheme 2

	reacn step										total
	1	2 ^a	3 ^b	4 ^c	5 (TS)	6	7	8 ^d	9	10	
ΔE (kcal/mol), large basis, gas phase	0	1 [-6.0]	15	33	38.6	24.5	18.4	36.2	-5.8	-18.9	-14.3
ΔE (kcal/mol), large basis, solvent	0	4 [-6.6]	17	30	35.1	21	13	30	-7	-24	-26
ΔG_{corr} (kcal/mol)	0	4.1 [-4.4]	17.7	14	18.2	3.6	-5.7	10	-9.4	-26.5	-27.8

^a The energy in brackets corresponds to the catalyst–substrate adduct with the alcohol coordinated in the second coordination sphere of Pd. ^b Energy of the intermediate complex without the vacant coordination site on Pd (Figure 2B): the vacant site is filled by pyridine. ^c The energy of the three-coordinated complex? ^d DFT/UB3LYP, triplet ground electronic state without accounting for the spin–orbit effect. Spin–orbit interaction will lower the energy of the complex.

constrained at the equilibrium distance delivers the complex 8.8 kcal/mol (B3LYP/lacvp*, gas phase) higher than the true stable complex in Figure 8B with H₂O₂ and AcO.

8. Total Energy Profile of the Reaction with the Palladacycle 1

The oxidation reaction under study is quite complex, and for obvious reasons we have broken it down to a sequence of simple steps. Few assumptions were made about the order of these steps and about the coordination stereochemistry of Pd(II). Our computations indicate that during the oxidation part of the reaction (Scheme 3, Figure 9) Pd(II) prefers a square-planar coordination geometry. For example, attempts to optimize the geometry of the Pd hydride complex with AcOH instead of pyridine were successful, but AcOH was replaced by pyridine when both units were included in the geometry optimization. We have also found that at our level of theory molecular oxygen does not form adducts with four-coordinated Pd hydride complexes (such as that from step 5, Scheme 3).

We believe that the O₂–Pd hydride complex (see Figure 7A,B) provides a realistic model for the Pd–oxygen interaction. We have looked at the possibility of binding of AcOH to this palladium–hydride–oxygen complex and found that the electronic binding energy of AcOH to the Pd–O₂ complex is rather small, 3.54 kcal/mol, at the triplet state.

The total energy profile for the catalytic cycle is summarized in Table 1.

Solvent effects on the total energy of the reaction steps are small. A Gibbs free energy profile of the reaction with the corresponding Pd complexes is presented in Figure 9. Formation of the alcohol–palladium adduct complex with the alcohol in the second coordination sphere is a favorable initiation of the reaction (green bar in Figure 9). The transition state and the reaction profile correspond to a dissociative reaction pathway, which necessarily proceeds via the three-coordinated Pd intermediate (see Figures 5, 6, and 9) where the pyridine dissociates completely prior to the rate-limiting step, β -hydride elimination. Our model implies that pyridine is a spectator during the β -hydride elimination process.

An alternative pathway implies weak coordination of the ligand, i.e., pyridine, to Pd(II) in the transition state.^{8c} Entropy contribution plays an important role in the Gibbs free energy profile of the reaction with a variable number of ligands per reaction step. Accounting for the thermochemical effects, namely for the increase of entropy, makes pyridine unbound (steps 3 and 4 in Table 1). Entropy effects, namely translational contributions, are certainly overestimated in the model with free pyridine, and therefore they are also highly sensitive to solvent effects. We expect that the energies of the reaction steps 3 and 4 provide upper and lower estimates for the “true” energy of the precursor to the β -hydride elimination. In the associative type of the β -hydride elimination, the pyridine molecule may stay in the second coordination sphere with a rather weak bond to Pd; despite all our efforts, we were not able to locate a transition state for the associative reaction pathway with the pyridine bound to the Pd complex in the second coordination sphere. Dissociation of pyridine prior to β -hydride elimination affects the relative Gibbs free energy of the transition state (compare ΔE and ΔG from Table 1, step 5). It is conceivable that our model of the dissociative transition state is oversimplified, and therefore the relative electronic energy, ΔE , of the transition state provides an upper estimation of the activation energy.

9. Conclusions

We have performed a complete computational study of the catalytic cycle for oxidation of a secondary alcohol to the corresponding ketone via the β -hydride elimination intermediate. The model also includes the second part of the cycle where oxygen interacts with the Pd(II) intermediate. Our main findings are as follows:

1. We have identified a common motif, an O–H interaction, in the binding of the substrate to different types of catalytic complexes.

2. β -Hydride elimination is the rate-limiting step (the corresponding transition state is the highest point on the potential profile),

3. The β -hydride elimination pathways for the palladacycle **1** and for Uemura’s catalytic system are shown to proceed via similar transition states.

4. The formation of AcOH is strongly endergonic at the very first deprotonation step (formation of the alkoxide). Therefore, addition of AcOH to the system inhibits the oxidation rate by effective back-protonation of the alkoxide.

5. According to the computed reaction energy profile, oxygen reduction is not rate limiting. We have identified a few possible O₂–Pd intermediates along this part of the reaction.

We have identified and compared β -hydride elimination transition states for the catalytic system involving palladacycle **1** and Uemura’s system. Our findings agree with the available experimental information about the rate-limiting step and with the experimentally studied/verified reaction pathway for a broad range of oxidative/catalytic systems.

Acknowledgment. We thank Dr. Sari Paavola and Prof. Margareta Blomberg for fruitful discussions. The Swedish National Allocation Committee (SNAC) is acknowledged for allocation of the computer time at the National Supercomputer Center (NSC), Linköping, Sweden.

Supporting Information Available: Tables giving coordinates, energies, and structural parameters of optimized complexes. This material is available free of charge via the Internet at <http://pubs.acs.org>.

OM049141Q